Optical absorption of wide quantum wires

A. N. Forshaw and D. M. Whittaker
Department of Physics, University of Sheffield, S3 7RH United Kingdom
(Received 8 April 1996)

We have calculated absorption spectra of quantum wires with rectangular cross-section and finite barrier height, accounting for the Coulombic mixing between subbands. Our method gives high-resolution spectra for both the bound and continuum states. We use these spectra to investigate the exciton binding energy and oscillator strength as a function of confinement, particularly discussing the quasi-one-dimensional (1D) to quasi-2D transition which occurs when one of the wire dimensions is increased. The spectra show Fano resonances in the continuum region, caused by the resonant coupling between discrete and energetically degenerate continuum states. The Fano resonance is characterized by an asymmetrically broadened peak and a dip below the level of the surrounding continuum. The broadening of these peaks is typically in the region of 1 meV. [S0163-1829(96)08035-6]

I. INTRODUCTION

As the fabrication and optical spectroscopy of quantum wires become more reliable, it is increasingly desirable to develop an understanding of excitonic behavior in such structures. Excitonic effects in quantum wells are well documented—see Winkler[1] for a comprehensive review, but as yet few calculations for quantum wires have been published. Variational methods have been used to calculate exciton binding energies, oscillator strengths, and wave functions,[2] but are limited in that they can only be used for the ground state. Glutsch and Bechstedt[3,4] have investigated the effects of excitons on the optical spectra of quantum wires, assuming complete confinement in one direction. Lefebvre *et al.*[5] recently described a fractional-dimensional space method to calculate analytically excitonic absorption, but considered only a single pair of subbands. However, as the size of fabricated wires is typically large compared with the exciton radius, the Coulomb mixing is large, rendering calculations nontrivial. In this paper we account for the effects of mixing many subbands, and confirm that although the single subband approximation works well for narrow quantum wires, it is less accurate for structures of realistic size. Glutsch and Chemla[6] also found this to be true.

In the simplest model of optical absorption, electrons are photoexcited from valence subbands to conduction subbands, and the various transitions can be classified by the subband numbers, e.g., $e1hh1$, $e1hh3$, $e2hh2$. The Coulomb interaction, however, couples all the electron and hole subbands with very important consequences.[3] Below the subband edges, quasibond states are formed, leading to distinct exciton peaks in the absorption spectra. At higher energies the Coulomb coupling also leads to a modification in the absorption in the continuum part of the spectrum.

In this paper we present theoretical high-resolution optical spectra for quantum wires. Our method, which has previously been applied to quantum wells[7] and superlattices[8] is essentially numerically exact, and has the distinct advantage of handling both discrete and continuum states in a single treatment.

For the present investigation we consider only heavy-hole to conduction-band transitions, in a wire with rectangular cross section and finite barrier heights. We are not so interested in making comparisons with experiment as with investigating the sort of behavior which would be observed in a high-quality quantum wire. In particular, we examine the evolution of excitons from the quasi-1D to nearly 2D situations by varying one of the wire dimensions. We have examined this size transition by studying the changes in binding energy, oscillator strength, and degree of subband mixing as the confinement is reduced.

Our spectra also exhibit Fano resonances.[9] These are due to the resonant coupling, via the Coulomb interaction, of discrete states from higher energy subbands and continuum states from lower-energy subbands. The Fano line shapes are characterized by their asymmetric broadening, accompanied by a dip below the level of the surrounding continuum. These have been predicted analytically[10] as a general feature of both quantum-well and quantum wire optical absorption spectra, and have also been observed in previous numerical calculations.[7] Fano resonances have been observed experimentally in asymmetric double quantum wells[11] but not in quantum wires.

II. THEORY

We consider a quantum wire in which carriers are confined by a finite potential in the (x,y) plane and are unbounded in the z direction. Working in the effective-mass approximation, the Hamiltonian for an electron-hole pair is of the form

$$H_{\mathrm{ex}}=\frac{\mathbf{p}_e^2}{2m_e}+\frac{\mathbf{p}_h^2}{2m_h}-\frac{e^2}{\epsilon_r|\mathbf{r}_e-\mathbf{r}_h|}+V_e^{\mathrm{wire}}(x_e,y_e)+V_h^{\mathrm{wire}}(x_h,y_h). \tag{1}$$

Here, $V_e^{\mathrm{wire}}(x_e,y_e)$ and $V_h^{\mathrm{wire}}(x_h,y_h)$ are the confining potentials for electron and hole, and ϵ_r is the dielectric constant. The uncoupled electron and hole states ϕ_i^e,ϕ_j^h and their corresponding eigenvalues $\varepsilon_i^e,\varepsilon_j^h$ are calculated by expressing the decoupled (x,y) problems as difference equations, and by using inverse iteration[12] to solve on a finite mesh. We

use this general method so that future calculations using realistic wire geometries may be performed. The exciton wave function is then expressed in the basis of the products of the uncoupled electron and hole states

$$\Psi_{\rm ex}(x,y,z)=\sum_{ij}\ \psi_{ij}(z)\,\phi_i^e(x,y)\,\phi_j^h(x,y). \tag{2}$$

$\psi_{ij}(z)$ describe the relative motion of the electron and hole in the axial direction, and are the solutions to a set of coupled differential equations,

$$-\frac{\hbar^2}{2\mu}\frac{d^2}{dz^2}\,\psi_{ij}(z)+\sum_{i'j'}\,V_{iji'j'}(z)\,\psi_{i'j'}(z) =(E-\varepsilon_i^e-\varepsilon_j^h)\,\psi_{ij}(z). \tag{3}$$

Here, $z=z_e-z_h$, μ is the reduced electron-hole mass, and E is an eigenvalue of the system. The Coulomb coupling between the ij and $i'j'$ pairs of subbands is given by the effective potential

$$V_{iji'j'}(z)=-\frac{e^2}{\epsilon_r}\int\int\int\int dx_e dx_h dy_e dy_h\,\frac{\phi_i^{e*}(x_e,y_e)\,\phi_{i'}^e(x_e,y_e)\,\phi_j^{h*}(x_h,y_h)\,\phi_{j'}^h(x_h,y_h)}{[(x_e-x_h)^2+(y_e-y_h)^2+z^2]^{1/2}}. \tag{4}$$

Because the mixing between subbands decreases as their separation increases, the infinite set of equations (3) can be truncated by ignoring subbands which are further than $\sim$50 meV from the subband edge. This is justified numerically by testing for convergence of the calculated exciton binding energy as a function of the number of subbands used. We now have a set of equations which could, in principle, be solved for all the exciton eigenstates, which in turn could be used to derive the optical absorption strength. However, our approach, a generalization of Zimmerman's method,[13] makes it unnecessary to solve for the eigenstates. The Green's-function method can be most easily illustrated by considering a single pair of subbands. In this case the exciton states are the eigenstates of

$$H\psi_\lambda=E_\lambda\psi_\lambda, \tag{5}$$

where

$$H(z)=-\frac{\hbar^2}{2\mu}\frac{\partial^2}{\partial z^2}+V_{1111}(z) \tag{6}$$

and

$$\psi_\lambda=\psi_{11}(z). \tag{7}$$

Rather than solve this equation, a Green's function is used. This is defined as the solution to the inhomogeneous equation

$$[H(z)-E]G(z,z',E)=\delta(z-z'). \tag{8}$$

The Green's function can be expanded in terms of the eigenstates of Eq. (5) using

$$G(z,z',E)=\sum_\lambda\ \frac{\psi_\lambda^*(z')\,\psi_\lambda(z)}{E_\lambda-E}. \tag{9}$$

Therefore the function

$$\lim_{\delta\to0}\ {\rm Im}[\,G(0,0,E+i\,\delta)]=\sum_\lambda\ \frac{|\psi_\lambda(0)|^2}{E_\lambda-(E+i\,\delta)} \tag{10}$$

is proportional to the exciton absorption spectrum. Where E_λ is discrete it gives a series of δ functions of the correct strength, and where E_λ is continuous, it gives the required continuum. In practice, to obtain convergence, it is necessary to make δ small but nonzero. There is, therefore, an element of Lorentzian broadening in the calculated spectra. In order to calculate the spectrum (10), the Green's function is constructed from a linear combination of numerical solutions to the inhomogeneous equation (8) with the appropriate boundary conditions: at large z the solution becomes plane-wave-like, and as $z\to0$ the solution behaves like a regular solution. G must be continuous at $z=z'$, and the first derivative of G has a step of $+1$ at $z=z'$. These two conditions are sufficient to determine the coefficients of the linear combination, and thus calculate G.

The generalization to a set of N coupled equations is made by defining an N-component Green's function as the solution to the set of inhomogeneous equations

$$[H_{ij}(z)-E]G_{ij}(z,z',E)=f_{ij}\delta(z-z') \tag{11}$$

(i.e., one equation for each ij) where f_{ij} is the overlap integral associated with the ijth pair of subbands

$$f_{ij}=\int\int dx\ dy\,\phi_i^e(x,y)\,\phi_j^h(x,y). \tag{12}$$

In this case the eigenfunction expansion is

$$G_{ij}(z,z',E)=\sum_{i'j'}\ \sum_\lambda\ \frac{\psi_{\lambda,i'j'}^*(z')\,\psi_{\lambda,ij}(z)\,f_{i'j'}}{E_\lambda-E} \tag{13}$$

and the absorption spectrum is

$$\lim_{\delta\to0}\ {\rm Im}\left[\sum_{ij}\ G_{ij}(0,0,E+i\,\delta)\,f_{ij}^*\right]. \tag{14}$$

The Green's function is now numerically constructed out of N-independent solutions to the defining equation for large and small z, and the continuity and jump conditions are used to calculate the coefficients. This method enables efficient calculation of high-resolution spectra.

The prescription to calculate the spectral absorption therefore is to calculate the uncoupled electron and hole states, then evaluate the effective potential matrix elements

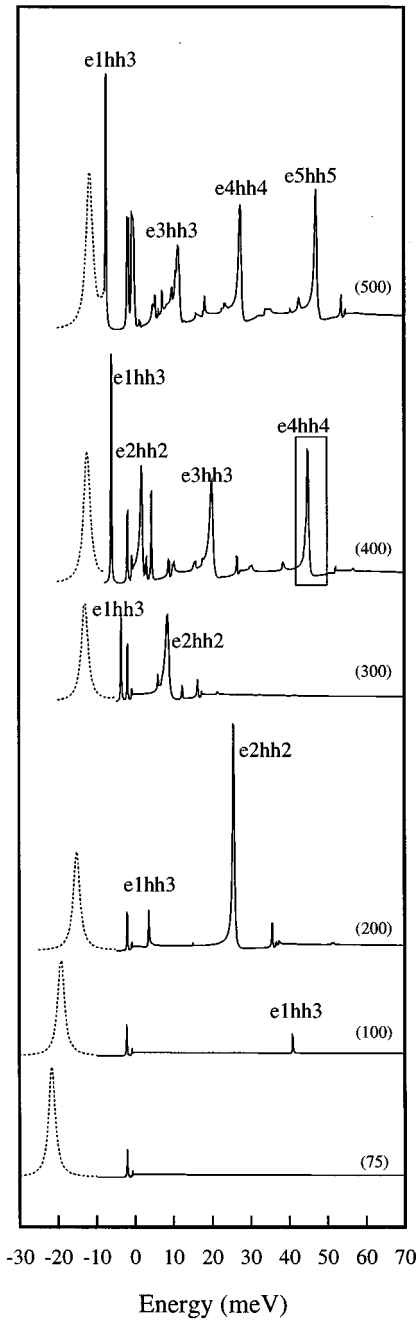

FIG. 1. Calculated absorption spectra for rectangular quantum wires, ranging from 50×75 Å to 50×500 Å. The dotted lines indicate the $e1hh1$ peak calculated with 1-meV broadening and the solid lines have been calculated with 0.1-meV broadening.

$V_{iji'j'}(z)$ which couple subband pairs, and finally to construct the Green's function for the system of equations (3).

III. RESULTS AND DISCUSSION

Figure 1 shows calculated absorption spectra for a range of rectangular quantum wires. In each case the width in the x direction is fixed at 50 Å, but the width in the y direction is varied from 75 to 500 Å (henceforth the word ''width'' refers to the width in the y direction). A small homogeneous broadening of 0.1 meV was used, but for clarity the exciton ground-state peaks (dotted lines) are shown with 1-meV broadening. The energy zero refers in each case to the $e1hh1$ subband gap. The material parameters used correspond to GaAs/$Al_{0.52}Ga_{0.48}As$ structures at 4.2 K, with a conduction to a valence-band offset ratio of 65:35. Just below the subband edge, excited exciton states of even parity are clearly visible. Above the subband edge, the strongest peaks are for the allowed transitions with $i=j$. However, other transitions are also apparent. The strongest of these is $e1hh3$ which despite having a small overlap mixes strongly with the allowed states via the Coulomb interaction. The mixing gets stronger in wider wires as $e1hh3$ moves closer to the $e1hh1$ state.

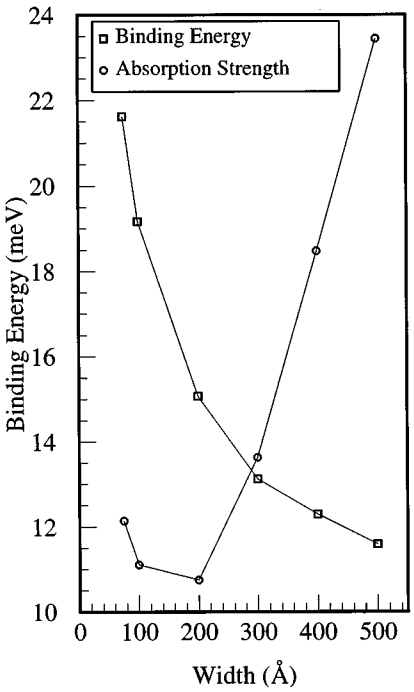

FIG. 2. Binding energy and oscillator strength of the $e1hh1$ transition as a function of wire size.

The binding energy and oscillator strength of the ground state are plotted as a function of wire width in Fig. 2. As expected, the binding energy decreases as the width is increased, due to a weakening effective potential. However, this is tempered by an increasing degree of subband mixing at large widths. As the subbands move closer together the axial correlation increases, which tends to enhance the binding energy. For example, in the 500-Å case, using a single pair of subbands in the calculation gives a binding energy of 9.6 meV, but adding as many pairs of subbands as is necessary for convergence leads to a binding energy of 11.6 meV. In the limit of infinite width we have a quantum-well situation where the discrete subbands caused by the confinement in the y direction have formed a continuous dispersion, and in which the binding energy of our calculation should agree with that of a quantum-well calculation using an appropriate effective potential. Of course, in the 500-Å wire we still see discrete subbands, but they are closely spaced and the binding energy of 11.6 meV is only slightly greater than that of 11.2 meV from the quantum-well calculation.

The oscillator strength of the ground state initially dips as the wire width is increased. This is because the expectation value of the electron-hole separation decreases with decreas-

ing confinement. As the width increases further, the oscillator strength increases as both the axial correlation and density of states increase. The behavior of the oscillator strength in this transition from strong to weak confinement has been previously discussed.[14,15] At large widths the increase is approximately linear, indicative of a 2D system in which the absorption is proportional to the size of the sample. In contrast, calculations ignoring the subband coupling predict a monotonic decrease in oscillator strength.

Examination of the $e1hh1$ bound-state wave function confirms this suggestion. The degree of subband mixing increases with increasing width. For the two smallest wires the wave function is made up almost entirely of the $e1hh1$ eigenstate, i.e., $\psi_{ij} \approx 0$ for $i,j \neq 1$. As the size increases the $e1hh1$ state remains the most significant, but even parity states such as $e1hh3$, $e2hh2$, $e3hh1$, etc., become more important in the sum of Eq. (2). In other words, we can think of the exciton as becoming more quantum-well-like as the confinement is reduced.

The spectra for wires with widths greater than 75 Å exhibit Fano resonances. These are caused by the resonant coupling of a discrete state of a higher-energy subband pair and energetically degenerate continuum states from lower subbands. The line shape of a Fano resonance has the functional form

$$\alpha(\epsilon) = \frac{(q+\epsilon)^2}{1+\epsilon^2} \tag{15}$$

where ϵ is an energy normalized relative to the resonance energy E_r of the discrete state,

$$\epsilon = \frac{E - E_r}{\Gamma/2}. \tag{16}$$

The absorption profile is thus characterized by the peak width Γ, and by the Fano parameter q, which gives the ratio of the transition matrix elements to the discrete state and to the continuum.

The widths of the peaks are much larger than the homogeneous broadening used in the calculation. Figure 3 shows a detailed view of the resonance in the frame box of Fig. 1. This feature fits the functional form very well using $q=-6$ and $\Gamma=0.6$ meV. For diagonal transitions ($i=j$, $i'=j'$) and electron-hole symmetry, the Fano parameter is always negative.[10] However, a general rule can not been made for the coupled case, and in our spectra the $e1hh3$ resonance in the 50×100 Å and 50×200 Å wires has a positive Fano parameter. Looking at the $e1hh3$ peak it is also clear that the asymmetry does arise from coupling to continuum states, as in the 300-, 400-, and 500-Å wires in which it forms a bound state below the continuum edge, the line shape is Lorentzian. For each wire the magnitude of q increases with increasing energy, indicating reduced coupling at higher order in agreement with the Fano model.

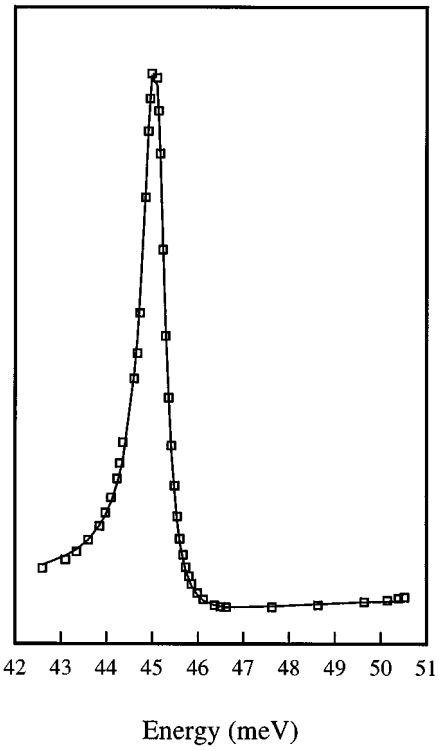

FIG. 3. Close up of the Fano resonance in the frame box of Fig. 1 (squares). The solid line represents the predicted functional form calculated with $q=-6.0$ and $\Gamma=0.6$ meV.

IV. SUMMARY

We have presented a method to calculate accurately excitonic spectra in quantum wires, and have described the transition of an exciton from confinement in two directions to confinement in just one dimension. We find that it is essential to consider the effects of subband mixing in order to obtain accurate results for the binding energy and oscillator strength in larger quantum wires. The binding energy is increased by the axial correlation of closely spaced subbands, and the oscillator strength rises at large widths. We also see Fano resonances in our spectra, with broadening in the region of 1 meV.

[1] R. Winkler, Phys. Rev. B **51**, 14 935 (1995).
[2] F. L. Madarasz, F. Szmulowicz, F. K. Hopkins, and D. L. Dorsey, Phys. Rev. B **49**, 13 528 (1994).
[3] S. Glutsch and F. Bechstedt, Phys. Rev. B **47**, 4315 (1993).
[4] S. Glutsch and F. Bechstedt, Phys. Rev. B **47**, 6385 (1993).
[5] P. Lefebvre, P. Christol, H. Mathieu, and S. Glutsch, Phys. Rev. B **52**, 5756 (1995).
[6] S. Glutsch and D. S. Chemla, Phys. Rev. B **53**, 15 902 (1996).
[7] A. R. K. Willcox and D. M. Whittaker, Superlattices Microstruct. **16**, 59 (1994).
[8] D. M. Whittaker, Europhys. Lett. **31**, 55 (1995).
[9] U. Fano, Phys. Rev. **124**, 1866 (1961).
[10] S. Glutsch, D. S. Chemla, and F. Bechstedt, Phys. Rev. B **51**, 16 885 (1995).
[11] D. Y. Oberli, G. Böhm, G. Weimann, and J. A. Brum, Phys. Rev. B **49**, 5757 (1994).

[12] W. H. Press, S. A. Teukolsky, W. T. Vetterling, and B. P. Flannery, *Numerical Recipes In FORTRAN* (Cambridge University Press, Cambridge, 1992).
[13] R. Zimmermann, Phys. Status Solidi B **135**, 681 (1986).
[14] A. D'Andrea and R. DelSole, Solid State Commun. **74**, 1121 (1990).
[15] L. C. Andreani, A. D'Andrea, and R. DelSole, Phys. Lett. A **168**, 451 (1992).